

# Laser Speckle Reduction Using a Liquid Crystal Diffuser Enhanced with Redox Dopants

Yihan Jin,\* David J. Hansford, Steve J. Elston, and Stephen M. Morris\*


Herein, a large reduction in the speckle noise is observed using a thin electroresponsive film consisting of a chiral nematic liquid crystal (LC) that has been enhanced with the addition of a redox dopant. Two different redox dopants are investigated over a range of concentrations, one being an electron acceptor and the other being an electron donor redox dopant. Results are presented that show that the incorporation of either of these dopants leads to a greater reduction in the speckle contrast than that observed using just the chiral nematic LC host when subjected to electrohydrodynamic instabilities. Furthermore, it is found that the permanent electrochemical reactions typically observed when ionic dopants, such as cetyltrimethylammonium bromide, are used are not observed for these devices, resulting in a considerable improvement in terms of the operating lifetime of the speckle reducer technology. To conclude, results that show that the speckle contrast can be reduced to  $C = 0.11 \pm 0.02$  at a temperature of 30 °C are presented and the improvement of the quality of an image generated using a modified commercial projector fitted with a monochromatic laser source is demonstrated.

## 1. Introduction

Laser speckle is a well-known optical phenomenon that has been investigated extensively since the invention of the laser. It consists of a random pattern of bright and dark spots superimposed on an image, which can limit the overall quality of the perceived image. The degree of speckle present in a projected image with uniform average intensity can be quantified by the speckle contrast,  $C$ , of the interference pattern.<sup>[1]</sup> This parameter, which was introduced by Goodman, takes the form

$$C = \frac{\sigma_I}{\bar{I}} \quad (1)$$

Y. Jin, Dr. D. J. Hansford, Prof. S. J. Elston, Prof. S. M. Morris  
Department of Engineering Science  
University of Oxford  
Parks Road, Oxford OX1 3PJ, UK  
E-mail: yihan.jin@eng.ox.ac.uk; stephen.morris@eng.ox.ac.uk

 The ORCID identification number(s) for the author(s) of this article can be found under <https://doi.org/10.1002/adpr.202000184>.

© 2021 The Authors. Advanced Photonics Research published by Wiley-VCH GmbH. This is an open access article under the terms of the Creative Commons Attribution License, which permits use, distribution and reproduction in any medium, provided the original work is properly cited.

DOI: 10.1002/adpr.202000184

where  $\sigma_I$  is the standard deviation in the intensity and  $\bar{I}$  is the average intensity value.

Methods for reducing  $C$  are typically based on the concept that when two or more statistically independent (or partially decorrelated) speckle patterns are superimposed, the random intensity fluctuations will be “averaged out” across the image.<sup>[1]</sup> In accordance, speckle reduction techniques can be separated according to whether the statistically independent speckle patterns are created instantaneously or time sequentially. Time-sequential methods take advantage of the finite integration time of the observer, enabling the speckle to be substantially reduced for a human viewer. Speckle reduction techniques can be further classified in terms of how these speckle patterns are mutually decorrelated, e.g., spectral decorrelation, spatial decorrelation, angular decorrelation, and polarization decorrelation.<sup>[1]</sup> As an example,

spectral decorrelation involves using two or more independent monochromatic sources with wavelengths  $\lambda_1$  and  $\lambda_2$  to illuminate a screen from the same position and angle, leading to two speckle patterns that are decorrelated as a result of the wavelength variation  $\Delta\lambda$ . This decorrelation increases with  $\Delta\lambda$ .

Speckle reduction using spectral decorrelation techniques can also be achieved through wavelength chirping, whereby the wavelength of the laser emission is varied within the integration time of the detector (such as the eye). Alternatively, for spatial decorrelation methods, the objective is to make the spatial resolution larger than the size of the coherence area so that the “spots” in the speckle pattern are blurred together. With this in mind, researchers have used random lasers with low spatial coherence and therefore very small coherence areas at the screen.<sup>[2]</sup> Speckle contrast can also be reduced instantaneously by illuminating the screen with multiple light sources simultaneously that vary in illumination angle. The greater the variation in angle between sources, the more decorrelated the resulting speckle patterns will be. A time-sequential variation in angle can also be achieved by passing light through a moving rotating ground glass diffuser (RGGD), which is the most common way to reduce the speckle contrast.<sup>[3–5]</sup>

By virtue of their electro-optic properties, liquid crystals (LCs) are appealing for the reduction of the speckle contrast and as a result have been considered for this purpose by numerous research teams.<sup>[6–15]</sup> An example of previous research in this area involved the use of a nematic LC device with a controllable

alignment layer consisting of polyvinyl alcohol (PVA) and an azo dye.<sup>[6]</sup> Exposing the device to ultraviolet (UV) light resulted in a reorientation of the LC director through the PVA/azo dye alignment layer enabling access to two orthogonal polarization states and thus giving rise to a reduction in the speckle contrast of  $1/\sqrt{2}$ .<sup>[6]</sup> A greater reduction in speckle was observed by Andreev et al., which involved the use of a ferroelectric LC (FLC) to create a spatially and temporally random refractive index across the cell, leading to a speckle reduction of 50%.<sup>[7–9]</sup> Similarly, Furue et al. have also reported speckle reduction using FLCs that are either surface or polymer stabilized as well as the use of nematic LCs dispersed with a photocurable monomer.<sup>[10,11,13]</sup> Other techniques have included the addition of nanoparticles to LC materials.<sup>[14,15]</sup> Alternatively, LC spatial light modulator (SLM) technology has been used to generate multiple random phase masks corresponding to the Hadamard orthogonal functions.<sup>[12]</sup> This approach has been shown to reduce speckle contrast by  $1/\sqrt{64}$  when using 64 cyclic phase patterns. Although the improvement in speckle reduction is impressive, the drawback with this approach is the need for an expensive and bulky SLM.

To overcome these issues, we have developed a method that takes advantage of the rapid, random movement of the local director in a chiral nematic LC so as to construct a compact electroresponsive diffuser that is capable of combatting speckle noise.<sup>[16]</sup> In our previous study, we showed that by dispersing an ionic dopant in the form of cetyltrimethylammonium bromide (CTAB) into a positive dielectric anisotropy chiral nematic LC mixture, the speckle contrast was found to be reduced. Briefly, when a He–Ne laser was used to illuminate a white screen a value of  $C = 0.67–0.70$  was recorded, which was decreased to  $C = 0.22 \pm 0.02$  with the addition of our LC diffuser when subjected to a simple, low-frequency (150–450 Hz) square-wave electric field.

Our technology is based upon the approach of exploiting time-sequential angular decorrelation, which is obtained through the rapid, random movement of anisotropic molecules in the LC diffuser. Chiral nematic LCs are known to exhibit a highly scattering, stationary focal conic state, which has been used previously for the optical storage of information.<sup>[17]</sup> By applying an electric field to this LC diffuser, turbulence can be induced in the form of electrohydrodynamic instabilities (EHDIs). In this case, the conductivity and dielectric anisotropy can be used to impose competing torques on the LC director, which creates instabilities in the macroscopic alignment. As the voltage is further increased, focal conic domains are formed that become more agitated by the increasing flow velocity until, above a larger threshold voltage, the flow becomes turbulent and completely disordered. In this state the director is randomly aligned in both space and time. This causes the material to become highly scattering, appearing opaque and with a milky-white appearance to the eye. Short-pitch chiral nematic LCs appear to be best suited for speckle reduction, with pitch values below  $1\ \mu\text{m}$  being capable of reducing the speckle contrast to  $C = 0.22 \pm 0.02$  for  $\lambda = 632\ \text{nm}$ .<sup>[18]</sup>

To boost EHDI, ions can be introduced to the LC mixture through charge injection at the electrodes or by adding specific ionic dopants. The motion of these ions through the LC can cause turbulence. To encourage instability in the LC, researchers

have investigated different approaches, such as the use of ionic dopants in the form of CTAB or redox dopants.<sup>[16,19]</sup> In our previous work, even though the reduction in the speckle contrast was encouraging, the degradation of the CTAB-doped thin films at high electric field amplitudes, due to the irreversible electrochemical reactions that occur at the electrodes, can limit their use in practical applications.<sup>[20]</sup> Proposed ideas for related applications involving ionic dopants in LC materials have included the enhancement of the functionality of smart windows.<sup>[21,22]</sup>

Redox dopants, on the other hand, are renowned for their electrochemical properties as they can be selected to improve the stability as well as maintain or even improve the dynamic scattering characteristics of liquid-crystalline materials.<sup>[19,23]</sup> These dopants can be classified as being either 1) donors or 2) acceptors, and there has been considerable recent interest in their use with LCs to enhance device functionality.<sup>[24–26]</sup> Unlike ionic dopants, these redox dopants readily undergo reversible electrochemical reactions at the electrodes. The purpose of this study, therefore, is to consider the impact of using redox dopants instead of conventional ionic dopants such as CTAB and to demonstrate an improvement in the operating lifetime of an LC diffuser when subjected to a range of electric field conditions. To enhance the conductivity properties and avoid permanent electrochemical deterioration in the diffuser, a redox dopant in the form of 7,7,8,8-tetracyanoquinodimethane (TCNQ) or *p*-phenylenediamine (PPD) (see Figure 1) was added at different concentrations by weight to a chiral nematic LC mixture.<sup>[27,28]</sup> TCNQ and PPD are examples of electron acceptor and donor species, respectively, that can effectively increase the density of current carriers (ionic charges).<sup>[19]</sup>

## 2. Results and Discussion

### 2.1. LC Speckle Reducer Without Dopants

To characterize the speckle reducer, we developed an automated system that records the speckle contrast in real time and is configured in accordance with the recommended practice for the measurement of speckle in laboratory conditions as defined by the Laser Illuminated Projector Association (see Figure 2 and Experimental Section).<sup>[29]</sup> Examples of the speckle patterns captured on the CCD camera without and with the LC diffuser are shown in Figure 3a,b. For this example, the mixture consisted of the nematic LC BL006 (Merck) and 3.0 wt% of the high-twisting power chiral dopant R5011 (Merck). The mixture was found to have a pitch of  $p \approx 310\ \text{nm}$  at  $30\ ^\circ\text{C}$  and the peak speckle reduction electric field conditions were found to occur at  $E_p = 15.3\ \text{V}/\mu\text{m}$  and  $f_p = 38\ \text{Hz}$ , where  $E_p$  and  $f_p$  are,

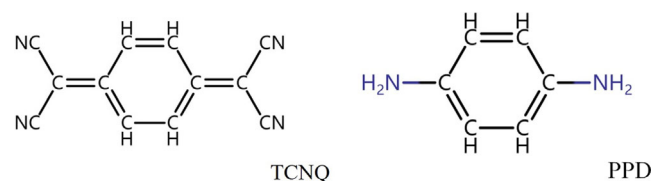


**Figure 1.** The chemical structures of the redox dopants considered in this study, TCNQ and PPD.

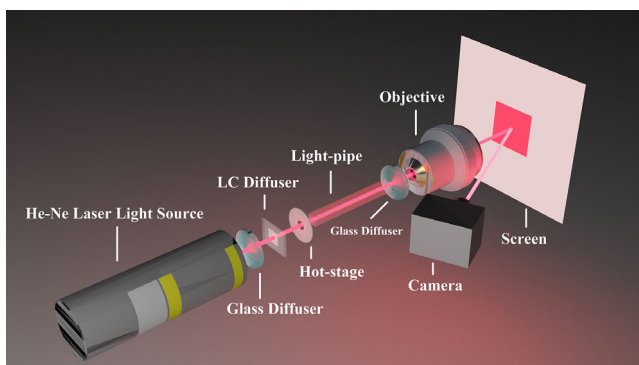


**Figure 2.** Illustration of the experimental arrangement used in this study to measure the speckle contrast,  $C$ .

respectively, the electric field and frequency at which peak speckle reduction is obtained.

To illustrate how the speckle contrast varies with the electric field parameters (i.e., amplitude and frequency) applied to the LC diffuser, Figure 3c,d shows the results for our base mixture (without redox dopants) in the form of color maps. Figure 3c shows the result for a low-resolution test used to identify (approximately) the field parameters where the maximum reduction in speckle contrast is observed. Results are presented for electric

field amplitudes ranging from 10 to 20  $\text{V } \mu\text{m}^{-1}$  and frequencies from 20 to 100 Hz. In this case, no notable change was observed at field amplitudes below 10  $\text{V } \mu\text{m}^{-1}$ . It can be seen that the greatest reduction in the speckle contrast is observed for amplitudes around 15  $\text{V } \mu\text{m}^{-1}$  across frequencies from 20 to 80 Hz. The black boxed region in (c) and (d) identifies the electric field parameters for which the lowest speckle contrast was recorded. Across the range of frequencies shown here, the speckle contrast is found to reduce with increasing electric field amplitude up to the point when the helical structure unwinds, at which point all dynamic scattering ceases, as shown by the dark red regions in Figure 3c at field amplitudes above  $\approx 15 \text{ V } \mu\text{m}^{-1}$ . At higher field amplitudes the LC transforms to a homeotropic nematic LC alignment, so EHDI ceases and no speckle reduction is observed in this state.<sup>[18]</sup> Figure 3d is an example of a high-resolution scan conducted to find the precise field conditions at which the speckle contrast was minimized; in this case, the results show that the lowest speckle contrast was observed for an amplitude of  $E = 15.3 \text{ V } \mu\text{m}^{-1}$  and a frequency of  $f = 38 \text{ Hz}$ . This field amplitude is quite large because of the relatively short pitch ( $< 400 \text{ nm}$ ) of the chiral nematic LC used (hence a large unwinding field), and the frequency optimizes turbulence in the conductive EHDI regime while ensuring that an associated flicker is not visible to the human eye. The results shown in Figure 3, as well as subsequent results presented in this study, are generally

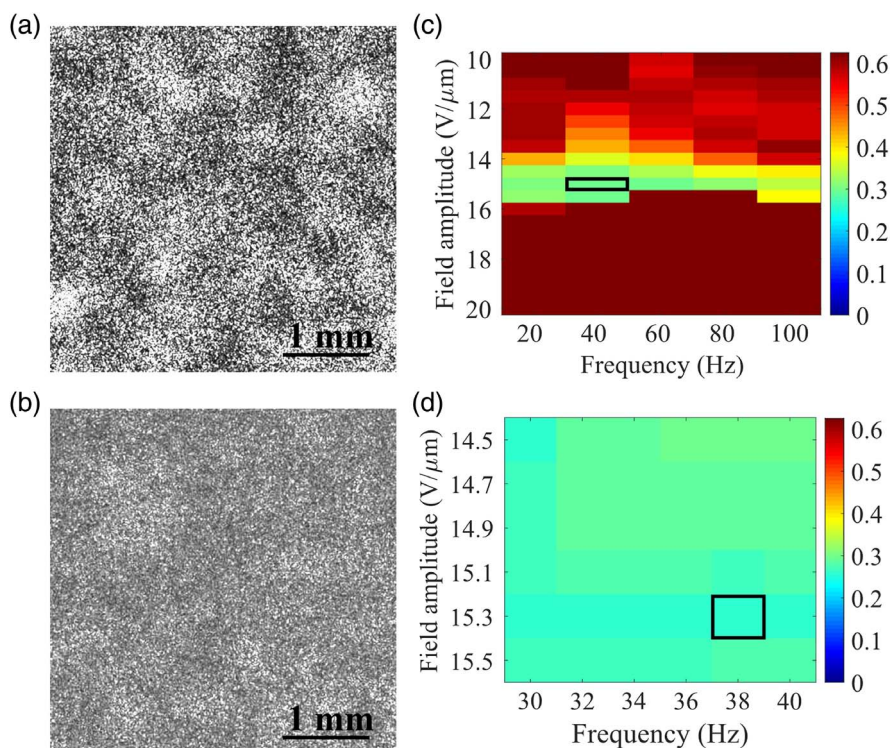


**Figure 3.** An example of the speckle pattern recorded by the CCD camera a) without the LC diffuser ( $C = 0.65 \pm 0.02$ ) and with b) the LC diffuser filled with BL006 + 3.0 wt% R5011 ( $C = 0.26 \pm 0.02$ ). Examples of a speckle contrast color map for the base mixture used in this study (BL006 + 3.0 wt% R5011), which shows the speckle contrast as a function of electric field amplitude and frequency under c) a low-resolution test and d) a high-resolution peak scan test. The black boxes in (c) and (d) highlight the minimum speckle contrast for each test, which is  $C = 0.29 \pm 0.02$  at  $E_p = 15 \text{ V } \mu\text{m}^{-1}$ ,  $f = 40 \text{ Hz}$  and  $C = 0.26 \pm 0.02$  at  $E_p = 15.3 \text{ V } \mu\text{m}^{-1}$ ,  $f = 38 \text{ Hz}$ , respectively. The experiments were taken at a temperature of  $30^\circ\text{C}$  and the cell thickness was  $20 \text{ } \mu\text{m}$ . The color bar on the right represents the legend for the speckle contrast. (a) Direct observation of the speckle pattern when no LC diffuser is in the path of the laser and (b) the speckle pattern observed from the region indicated by the black box in (d).

obtained at a temperature of 30 °C. This slightly elevated operating temperature was used to ensure that the operating conditions were consistent across all measurements and to avoid unwanted changes in the ambient room temperature.

## 2.2. LC Speckle Reducer with Redox Dopants

To determine the impact of the redox dopant on the speckle contrast and the electric field conditions for maximum speckle reduction, sweeps of the electric field amplitude and frequency were conducted for the base mixture consisting of BL006 + 3.0 wt% R5011 and 1.0 wt% of either redox dopant, TCNQ or PPD. For the purposes of comparison, measurements were also conducted for a sample consisting of 1.0 wt% of the ionic dopant CTAB. This concentration by weight was chosen for comparison because chiral nematic LC mixtures that contained the ionic dopant were found to degrade rapidly during testing if a concentration higher than 1.0 wt% was used. Other weight concentrations of the redox dopant are considered later in this study.

The results are shown in **Figure 4**, where it can be seen that the addition of either a redox or ionic dopant greatly increases the range of frequencies and field amplitudes over which speckle reduction is observed. In addition, for the samples including either the redox dopant, TCNQ, or the ionic dopant, CTAB, the field amplitudes required to observe the maximum reduction in the speckle contrast are found to occur at lower values. For example, the sample consisting of the 1.0 wt% TCNQ dopant, in particular, exhibits a reduction in the speckle contrast across almost all of the range of frequencies and field amplitudes

considered here, with the minimum speckle contrast (maximum speckle reduction) of  $C = 0.14 \pm 0.02$  being observed for an electric field amplitude of  $E = 15 \text{ V } \mu\text{m}^{-1}$  and a frequency of  $f = 30 \text{ Hz}$ . In comparison, for the base mixture, the minimum speckle contrast recorded was  $C = 0.26 \pm 0.02$ , which is noticeably higher than that observed for the sample doped with TCNQ. The sample containing the ionic dopant was found to exhibit an even lower speckle contrast of  $C = 0.11 \pm 0.02$  at a frequency of 100 Hz and a comparable electric field amplitude. However, it should be noted that this sample was rather unstable, as will be discussed further.

Once the minimum speckle contrast and corresponding electric field conditions had been determined for each sample, each one was then subjected to a 5 min steady-state response test every day for a period of 2 weeks. A plot of the minimum speckle contrast measured (at the peak field conditions) over this 2 week period can be seen **Figure 5a**, which shows the variation in the measured speckle contrast for the base chiral nematic LC sample as well as those consisting of either the acceptor or the donor redox dopant, PPD or TCNQ. Despite starting from a lower value of the speckle contrast, it is clear that the sample containing the ionic dopant, CTAB, deteriorates over time as the speckle contrast increases notably. By the end of the second week, the speckle contrast approaches the value recorded as if no LC diffruser was present in the experimental system (i.e.,  $C \approx 0.6$ ). At this point, due to the irreversible processes taking place, there is substantial degradation and oxidation of the LC inside the glass cell. The resultant significant changes in the composition of the LC mixture in the cell means that EHD no longer takes place under these operating conditions and the dynamic processes

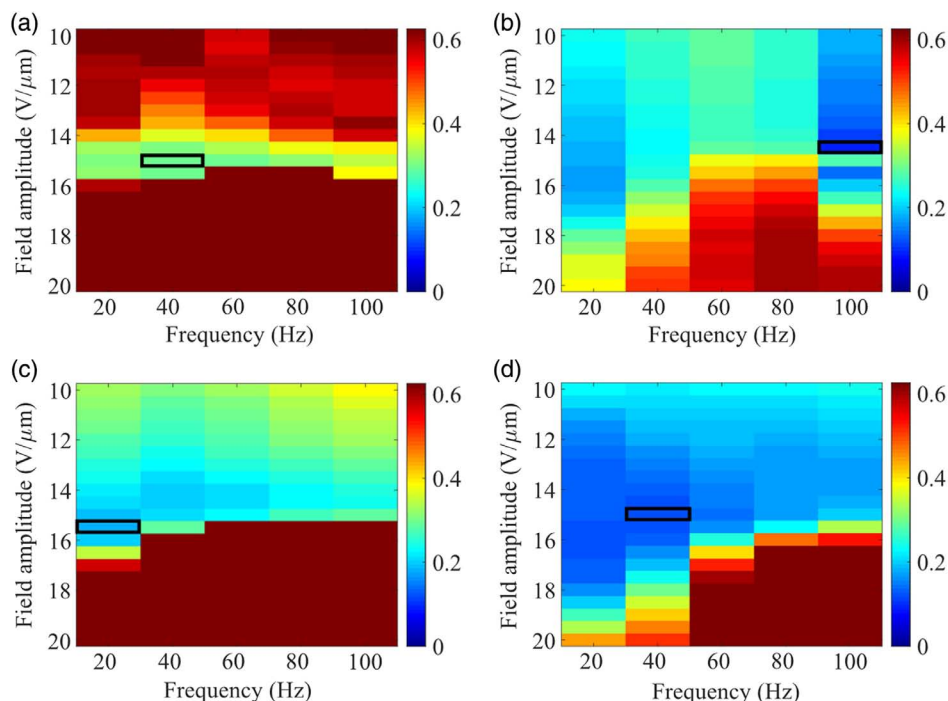


**Figure 4.** Color maps of the speckle contrast as a function of the electric field amplitude and frequency for the samples: a) base mixture (BL006 + 3 wt% R5011) (repeated here from Figure 3b for the purposes of comparison); b) base mixture + 1.0 wt% CTAB; c) base mixture + 1.0 wt% PPD; and d) base mixture + 1.0 wt% TCNQ. Measurements were conducted at a temperature of 30 °C and each sample was 20  $\mu\text{m}$  thick.



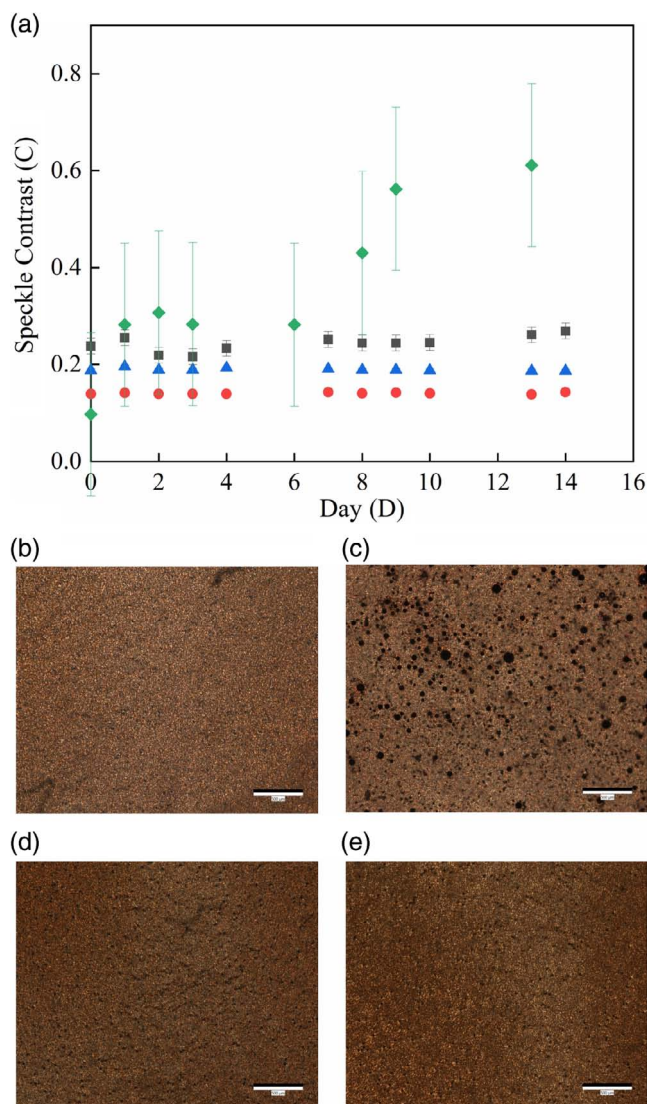


**Figure 5.** a) The speckle contrast as a function of number of days over 2 weeks. Data points represent the results for a 5 min steady-state response on each day for the following LC mixtures: BL006 + 3 wt% R5011 (black squares); BL006 + 3 wt% R5011 + 1.0 wt% CTAB (green diamonds); BL006 + 3 wt% R5011 + 1.0 wt% PPD (blue triangles); BL006 + 3 wt% R5011 + 1.0 wt% TCNQ (red circles). The pitch of the chiral nematic samples was  $p \approx 310$  nm and the measurements were conducted at a temperature of  $30^\circ\text{C}$ . The LC mixtures were capillary filled into  $20\ \mu\text{m}$  thick glass cells. Optical polarizing microscope images of the optical texture of the CTAB-doped mixture recorded on the b) 1st day and c) 14th day of testing are also shown. Optical polarizing microscope images of the optical texture of the BL006 + 3 wt% R5011 + 1.0 wt% TCNQ mixture recorded on the d) 1st day and e) 14th day of testing are also shown. Scale bars on the images are  $500\ \mu\text{m}$ .

cease. Therefore, the cell no longer functions as a speckle reducer, and so, the speckle contrast returns to the “unreduced” value of around 0.6. In contrast, for the base mixture and the two samples containing the redox dopants, there was very little change in the speckle contrast over time. Furthermore, the speckle contrast for the redox dopants shows a very flat response over the 2 week period and the low value of  $C = 0.14 \pm 0.02$  is

maintained throughout for the sample with the TCNQ redox dopant.

It is clear that with the addition of redox dopants to the base mixtures, the speckle contrast can be significantly reduced. In addition, due the reversible electrochemical reactions, devices containing redox dopants were able to perform better over time, especially compared with the CTAB-doped mixture. The CTAB-doped mixture did allow reduction of the speckle contrast to values closer to  $C = 0.10$  at room temperature, where the speckle pattern becomes almost imperceivable to the human eye; however, it is clear from the microscope images in Figure 5b,c that the sample degraded significantly within a short period of time. In comparison, it is evident from the microscope images in Figure 5d,e that the TCNQ-doped sample did not show any significant degradation.

Having demonstrated an improvement in the device performance with the addition of the redox dopants to the chiral nematic LC host, the next steps were to determine 1) the optimal concentration for the two different redox dopants; 2) to identify which redox dopant was able to reduce the speckle contrast to the lowest value at room temperature; and 3) how these mixtures performed over a period of continuous use. Toward this end, **Figure 6** shows the measured speckle contrast for mixtures consisting of either redox dopant (PPD or TCNQ) at concentrations by weight ranging from 0.2–2 wt%. It is clear from the figure, and in accordance with Figure 4 and 5, that the addition of either redox dopant results in a dramatic decrease in the speckle contrast, with the lowest values observed for mixtures consisting of  $<0.5$  wt% redox dopant. Specifically, at concentrations by weight of 0.2 wt%, the speckle contrast was found to be as low as  $C = 0.11 \pm 0.02$  for the sample containing the TCNQ dopant (which represents an  $\approx 60\%$  reduction in the speckle contrast compared to that observed for the base mixtures and an  $\approx 88\%$  reduction compared to that observed for no LC diffuser). For higher concentrations of dopant, irrespective of whether it is an acceptor or donor redox dopant, the speckle contrast was found to increase, but was still lower than that observed for devices fabricated using just the base mixture.

Figure 1 and 2, Supporting Information, show the variation in the speckle contrast,  $C$ , as a function of the electric field amplitude and frequency recorded for each concentration of redox dopant immediately after fabrication. The color maps make it clear that following fabrication the mixtures containing 0.2 wt% of either redox dopant are more desirable in terms of peak speckle reduction, although the range of field parameters over which speckle reduction is observed is found to increase with the concentration of dopant. Moreover, for all concentrations, it can be seen that the mixtures with the TCNQ dopant consistently outperform those containing PPD, in terms of both the minimum speckle contrast and the range of field parameters over which speckle reduction is observed.

For the sample that exhibited the lowest speckle contrast (BL006 + 3.0 wt% R5011 + 0.2 wt% TCNQ), we also investigated whether this low value for the speckle contrast could be maintained when the device was operated continuously over a period of time. For this experiment, a  $20\ \mu\text{m}$  thick device containing the aforementioned mixture was connected to a signal generator and voltage amplifier to apply an amplitude and frequency that matched the peak operating conditions ( $E_p$  and  $f_p$ ) for a

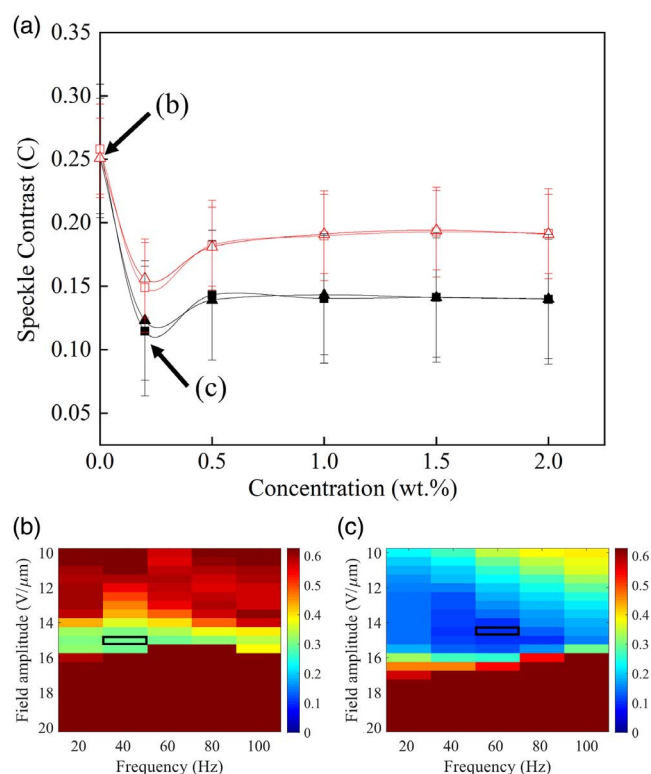


**Figure 6.** a) Plot of the speckle contrast,  $C$ , as a function of the concentration by weight of the redox dopant for samples consisting of BL006 + 3 wt% R5011 + PPD (red open symbols) and BL006 + 3 wt% R5011 + TCNQ (black solid symbols). Measurements conducted immediately after fabrication of each device are represented with square symbols, whereas measurements conducted 7 days after fabrication are represented with triangular symbols. b,c) Color maps of the speckle contrast showing the quick-scan result for the concentrations of redox dopant as labeled in (a). These represent the worst-case scenario with just the base mixture (b) and the best-case scenario with the 0.2 wt% TCNQ in the base mixture (c). The experiments were taken at a temperature of 30 °C and the cell thickness in each case was nominally 20 μm.

continuous period of 7 days. A measurement of the speckle contrast was then recorded each day, which involved conducting a high-resolution peak-scan test first to verify whether the  $E_p$  and  $f_p$  had drifted. As shown in Figure 7, the speckle contrast for both the base mixture (BL006 + 3.0 wt% R5011) and the best-performing redox-doped mixture (base mixture + 0.2 wt% TCNQ) increased with time but that of the redox-doped mixture plateaued at around  $C \approx 0.13$ . In all cases the values for the base mixture were much higher than that recorded for the redox-doped mixture.

### 2.3. Deployment in a Prototype Projector

To verify the performance of this LC speckle reducer technology in the setting of a practical application, photographs of images generated using a prototype projector system (modeled on a HITACHI CP-X250 Multimedia LCD Projector) with and without our LC technology were recorded. In this projector setup, the light source was a Coherent Genesis MX 561 SLM fiber laser

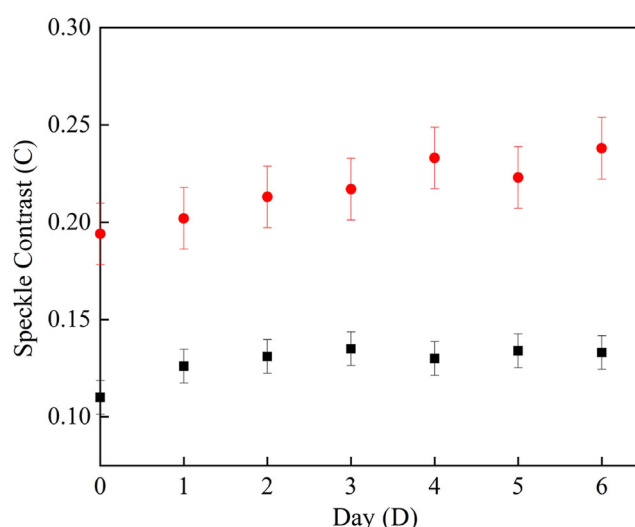


**Figure 7.** Plot of the speckle contrast as a function of the day number when the optimum mixture formulation (BL006 + 3.0 wt% R5011 + 0.2 wt% TCNQ, black points) was operated continuously over a period of 7 days. For the purposes of comparison, the red data points are data for the base mixture: BL006 + 3.0 wt% R5011 when operated continuously over the same period of time. The sample was held at a constant temperature of 30 °C for the duration of the 7 days and the sample thickness in each case was 20 μm.

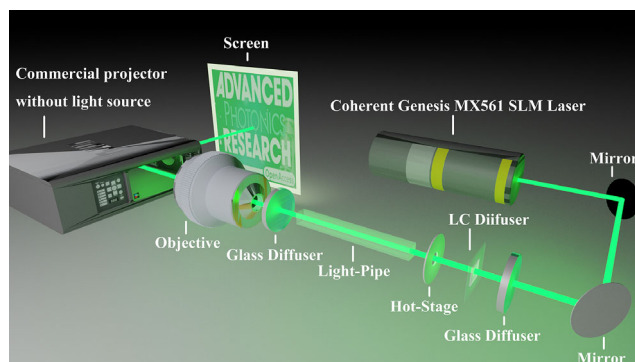


**Figure 8.** Schematic of the laser projector demonstrator.

with a wavelength of  $\lambda = 561 \pm 3$  nm and the resultant image was projected onto a white screen using the setup shown in Figure 8. In this case, the LC diffuser consists of the mixture (BL006 + 3.0 wt% R5011 + 0.2 wt% TCNQ) and the operating electric field conditions were  $E_p = 14.8$  V μm<sup>-1</sup> and  $f_p = 64$  Hz. Figure 9 shows the images observed on the screen with and without the LC diffuser. It is obvious that with the insertion of the LC diffuser, the resolution and features of the projected images are noticeably improved. With the insertion of the LC diffuser device, the speckle contrast was reduced by as much as 84%.

Even lower values of the speckle contrast can be obtained by operating the LC diffuser consisting of the optimal mixture BL006 + 3.0 wt% R5011 + 0.2 wt% TCNQ at a higher temperature of  $T = 55$  °C (Figure S3, Supporting Information). The results show that at this higher temperature the speckle contrast





**Figure 9.** Photographs of images generated using a prototype projector system (modeled on a HITACHI CP-X250 Multimedia LCD Projector): a,d,g) without our LC technology; b,e,h) with the LC diffuser operated under suboptimal electric field conditions; and c,f,i) with LC diffuser operated under optimal electric field conditions. The LC diffuser consisted of the mixture (BL006 + 3.0 wt% R5011 + 0.2 wt% TCNQ) filled into a nominally 20  $\mu\text{m}$  thick device. g–i) Journal logo reproduced with permission. Copyright Wiley-VCH.

could be reduced to  $C = 0.08 \pm 0.02$  and the performance was stable over a 60 min steady-state response test.

### 3. Conclusion

To conclude, in this work we have demonstrated that the addition of a redox dopant (0.2 wt% TCNQ) to a chiral nematic LC (composed of BL006 + 3.0 wt% R5011) can significantly reduce the speckle contrast perceived in a projected image from  $C = 0.65 \pm 0.02$  to  $C = 0.11 \pm 0.02$  at a temperature of 30  $^{\circ}\text{C}$  when imaging with a CCD camera with an integration time of 50 ms, chosen so as to emulate the response of the human eye. Two different redox dopants were considered (TCNQ and PPD) in this study, representing either an electron acceptor or electron donor type dopant. The dependence of the speckle noise reduction was investigated for chiral nematic mixtures containing these dopants at different concentrations by weight and were compared with devices that contained either an ionic dopant, such as CTAB, or no additional dopants.

Overall, when considered over a period of time there appears to be some dependence of the speckle reduction on the concentration of the redox dopant (for the range from 0.2 to 2 wt%), with the best performance observed for a concentration of 0.2 wt%. Also, it was found that for all concentrations considered the samples comprising the electron acceptor dopant exhibited the lowest speckle contrast values. Furthermore, the speckle reduction was considerably better with the addition of either redox dopant when compared to the performance of an LC diffuser consisting of just the base chiral nematic LC mixture. Unlike samples containing an ionic dopant, the performance was consistent over time, both when run intermittently over a 2 week period or when operated continuously for 7 days.

The LC diffuser device presented herein is tiny, portable, and easy to integrate into existing commercial systems that currently suffer from speckle noise. To highlight the ease with which the device can be integrated, we have demonstrated the notable improvement of an image generated using a commercial projector that was retrofitted with a monochromatic laser source and our LC diffuser technology. We believe that these findings would

be of significant interest for the development of laser projectors, laser microscopes, and laser holographic imaging systems.

## 4. Experimental Section

**Measurement System:** The experiment developed to measure the speckle contrast is shown in Figure 2. The coherent light source used to quantify the speckle contrast was a single-mode, continuous-wave, linearly polarized helium–neon laser (JDS Uniphase 1122 P,  $\lambda = 632.8$  nm). For these experiments, the power of the laser was kept sufficiently low so as not to influence the temperature of the LC sample under investigation. As shown in the figure, the light propagates through a 1500 grit glass diffuser, the LC diffuser mounted on a hot stage, a light pipe, a second 1500 grit glass diffuser, and a  $10\times$  microscope objective (Olympus UPlanFL N, NA = 0.3) before illuminating a projector screen (made from white paper). The purpose of putting a light pipe in the system was to ensure a uniform intensity profile. To capture the speckle pattern, but not impede the light path, the CCD camera was placed to the side of the projector screen at an angle of  $25^\circ$  between the normal direction of the screen and the CCD camera.

To control the operating temperature of the device, the LC diffuser was placed in a custom-made integrated hot stage connected to a controller (INSTEK MK1000) to guarantee a constant and steady temperature throughout each experiment. A monochrome CCD camera (QImaging Retiga R6 12 bit with  $1392 \times 1040$  pixels and  $4.65 \mu\text{m} \times 4.65 \mu\text{m}$  pixel size) was used to capture the speckle patterns. For these measurements a unity gamma correction was used so that the relationship between the optical intensity and pixel value was linear. If there was no such correction, the measured speckle contrast would change with the fluctuation and variation in the optical intensity. The intensity of the light reflected by the screen was adjusted to ensure the use of the full dynamic range of the CCD camera to avoid the loss of accuracy caused by discretisation errors. As the integration time for photopic vision at long wavelengths has a temporal integration time of the order of 50 ms, this value was used for the integration time of our camera.<sup>[30]</sup>

The speckle contrast of the He–Ne laser without an LC diffuser was tested and a measured value of  $C = 0.65 \pm 0.02$  was obtained, which is close to the theoretically expected value of  $1/\sqrt{2}$ . Equally, to benchmark the results for the LC device of this study, a rotating ground glass diffuser (RGGD) was inserted at the diffuser plane and tested for a rotation speed of 40–200 rpm, which was found to result in a speckle contrast of  $C = 0.04 \pm 0.02$  and is consistent with the data published elsewhere for similar RGGD-based systems.<sup>[31]</sup>

**Mixture Preparation:** In this study, the LC mixture consisted of the wide-temperature range nematic mixture BL006 (Merck Ltd), the chiral dopant R5011 (Merck Ltd), the redox dopants TCNQ and PPD (Sigma Aldrich), and the ionic dopant CTAB (Sigma Aldrich). To form a chiral nematic LC phase, the R5011 was dispersed in the nematic LC host, BL006, at a concentration by weight of 3.0 wt%. This resulted in a mixture with a pitch ranging from 298 to 328 nm (determined from the spectral location of the reflection band using an UV–vis spectrometer, Agilent Cary 8454 UV-Vis) at room temperature. The pitch was chosen based on the findings of previous work.<sup>[18]</sup> The mixtures were placed on a hot stage with a magnetic stirrer and were heated up to  $5^\circ\text{C}$  above the clearing point for a period of 24 h. After thermal mixing, the LC mixture was then filled via capillary action into commercially available INSTEK LC2 cells that have a nominal cell gap of  $d = 20.0 \mu\text{m}$ . Indium tin oxide (ITO) coatings of 23 nm on the inner substrates served as transparent electrodes and were patterned onto the inner sides of the glass substrates to create an active region of  $5 \text{ mm} \times 5 \text{ mm}$  at the centre of the cell. On top of the ITO layers were antiparallel rubbed polyimide layers. The cell gap was checked for each sample using an interference method with white light illumination at normal incidence. To examine whether the components had been dispersed uniformly, the LC cells were inspected on a polarizing optical microscope (Olympus BX51-P).

**Experimental Procedure:** An electric field was applied to the LC devices using a dual-channel function generator (Tektronix AFG 3022) and a voltage amplifier (FLC Electronics F10AD). To identify the optimum operating conditions where the speckle contrast would be reduced to a minimum value, each LC device was subjected to three separate tests. First, the speckle contrast was recorded by sweeping through a range of electric field amplitudes ( $10\text{--}20 \text{ V } \mu\text{m}^{-1}$  in increments of  $2 \text{ V } \mu\text{m}^{-1}$ ) and frequencies ( $20\text{--}100 \text{ Hz}$  in increments of  $10 \text{ Hz}$ ). This coarse sweep of the field parameters provided an estimation of the electric field conditions and frequency requirements required to achieve maximum speckle reduction. Based on this quick scan test assessment, the next step was to subject each device to a higher resolution scan to identify precisely the field parameters required for peak speckle reduction. In this peak scan test, the increments of the electric field and frequency were  $0.2 \text{ V } \mu\text{m}^{-1}$  and  $1.0 \text{ Hz}$ , respectively.

Finally, each LC device was subjected to a steady-state response test. For this, the signal generator was set to apply the electric field conditions corresponding to peak speckle reduction and the speckle contrast was recorded every 1 s continuously to determine the variation of the speckle contrast over a period of time. All of the tests mentioned earlier were conducted at  $30^\circ\text{C}$ . For the extended lifetime measurements, devices were operated at their peak speckle reduction electric field conditions for 2 weeks continuously, and the speckle contrast measurement system was set to record at regular intervals.

## Supporting Information

Supporting Information is available from the Wiley Online Library or from the author.

## Acknowledgements

The authors gratefully acknowledge the Engineering and Physical Sciences Research Council (UK) for financial support through the graduate studentship, EP/L505031/1, and Merck Ltd for providing the chiral dopant.

## Conflict of Interest

The authors declare no conflict of interest.

## Data Availability Statement

The data that support the findings of this study are available from the corresponding author upon reasonable request.

## Keywords

laser imaging, laser projection, liquid crystals, redox dopants, speckle reduction

Received: December 13, 2020

Revised: January 20, 2021

Published online: May 8, 2021

- [1] J. W. Goodman, *Speckle Phenomena in Optics: Theory and Applications*, Roberts & Company, Englewood, CO 2007.
- [2] B. Redding, M. A. Choma, H. Cao, *Nat. Photon.* **2012**, 6, 355.
- [3] G. Zheng, B. Wang, T. Fang, H. Cheng, Y. Qi, Y. W. Wang, B. X. Yan, Y. Bi, Y. Wang, S. W. Chu, T. J. Wu, J. K. Xu, H. T. Min, S. P. Yan, C. W. Ye, Z. D. Jia, *IEEE/OSA J. of Disp. Tech.* **2008**, 4, 314.
- [4] J. Li, *Microwave Opt. Technol. Lett.*, **2013**, 55, 138.



- [5] S. C. Shin, S. S. Yoo, S. Y. Lee, C. Y. Park, S. Y. Park, J. W. Kwon, S. G. Lee, *Displays*. **2006**, 27, 91.
- [6] K. Sueda, K. Tsubakimoto, N. Miyanaga, M. Nakatsuka, *Appl. Phys. Lett.* **2002**, 81, 5111.
- [7] A. A. Andreev, T. B. Andreeva, I. N. Kompanets, M. V. Minchenko, E. P. Pozhidaev, *J. Soc. Inf. Disp.* **2009**, 17, 801.
- [8] I. N. Kompanets, A. L. Andreev, T. B. Andreeva, M. V. Minchenko, *SID Sym. Digest Tech. Pap.* **2010**, 1065.
- [9] A. L. Andreev, T. B. Andreeva, I. N. Kompanets, *SID 2014 Dig.* **2014**, 31, 411.
- [10] H. Furue, A. Terashima, M. Shirao, Y. Koizumi, M. Ono, *Jpn. J. Appl. Phys.* **2011**, 50, 09NE14.
- [11] H. Furue, Y. Sugimoto, K. Iwami, W. Weng, M. Ono, *Mol. Cryst. Liq. Cryst.* **2015**, 612, 245.
- [12] J. I. Trisnadi, *Opt. Lett.* **2004**, 29, 11.
- [13] J.-H. Lin, S.-C. Chang, Y.-H. Li, C.-Y. Chien, C.-H. Chen, Y.-C. Lin, J.-J. Wu, S.-Y. Tsay, Y.-H. Chen, *Appl. Phys. Express* **2017**, 10, 031701.
- [14] H. Ishikawa, A. Shibase, W. Weng, M. Ono, H. Furue, *Mol. Cryst. Liq. Cryst.* **2017**, 646, 93.
- [15] J. Harden, K.-H. Chang, T. Seder, L. C. Chien, SPIE 11303, Emerging Liquid Crystal Technologies XV. **2020**, 113030O.
- [16] D. J. Hansford, J. A. J. Fells, S. J. Elston, S. M. Morris, *Appl. Phys. Lett.* **2016**, 109, 261104.
- [17] D. W. Berreman, W. R. Heffner, *SID 82 Digest*, **1982**, 242.
- [18] D. J. Hansford, Y. Jin, S. J. Elston, S. M. Morris, *Sci. Rep.*, **2021**, 11, 4818.
- [19] H. Sup Lim, J. D. Margerum, *Appl. Phys. Lett.* **1976**, 28, 478.
- [20] B. Gosse, J. P. Gosse, *J. Appl. Electrochem.* **1976**, 6, 515.
- [21] Y. Zhang, X. Yang, Y. Zhan, Y. Zhang, J. He, P. Lv, D. Yuan, X. Hu, D. Liu, D. J. Broer, G. Zhou, W. Zhao, *Adv. Opt. Mater.* **2020**, 2001465.
- [22] M. Mrkiewicz, P. Perkowski, M. Urbańska, D. Węglowska, W. Piecek, *J. Mol. Liq.* **2020**, 317, 113810.
- [23] A. A. Khan, S. M. Morris, D. J. Gardiner, M. Qasim, T. Wilkinson, H. J. Coles, *Opt. Mater.* **2015**, 42, 441.
- [24] S. Tokunaga, Y. Itoh, H. Tanaka, F. Araoka, T. Aida, *J. Am. Chem. Soc.*, **2018**, 140, 10946.
- [25] T. Szilvási, N. Bao, K. Nayani, H. Yu, P. Rai, R. J. Twieg, M. Mavrikakis, N. L. Abbott, *Angew. Chem. Int. Ed.*, **2018**, 57, 9665.
- [26] M. Funahashi, *Flex. Print. Electron.* **2020**, 5, 043001.
- [27] J. B. Torrance, B. A. Scott, F. B. Kaufman, *Solid State Commun.* **1975**, 17, 1369.
- [28] M. Sakamoto, B. Wasserman, M. S. Dresselhaus, G. E. Wnek, B. S. Elman, D. J. Sandman, *J. Appl. Phys.* **1986**, 60, 2788.
- [29] LIPA: RP – Speckle Measurement in Laboratory Conditions Version 1, <https://www.lipainfo.org/laser-illumination-sources/speckle-metrology/> (accessed: December 2020).
- [30] J. Krauskopf, J. D. Mollon, *J. Physiol.* **1971**, 219, 611.
- [31] M. N. Akram, X. Chen, *Opt. Rev.* **2016**, 23, 108.